Supporting Information

Trouillard et al. 10.1073/pnas.1109510108

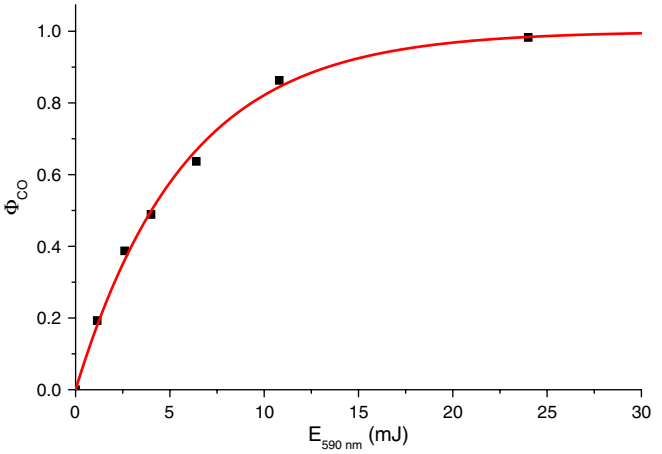

Fig. S1 Plot of the relative amount of photodissociated CO from heme a_3 of CcOx, as monitored by the intensity of the absorption increase at 445 nm 10 μs after the flash, against the flash intensity (black squares). The experimental data were fitted with an exponential function (red solid line).

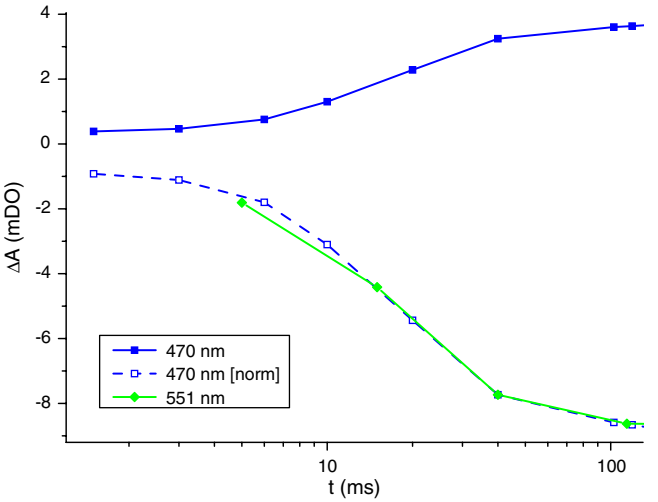

Fig. S2. Kinetics of cytochrome *c* oxidation under cytochrome bc_1 inhibited conditions [by Tri-Decyl Stigmatellin (TDS)], at 470 nm (blue solid line), 551 nm (green solid line), and 470 nm, normalized to show the kinetic equivalence with the 551 nm trace (blue dashed line); [O2] ~ 2.6 μM.

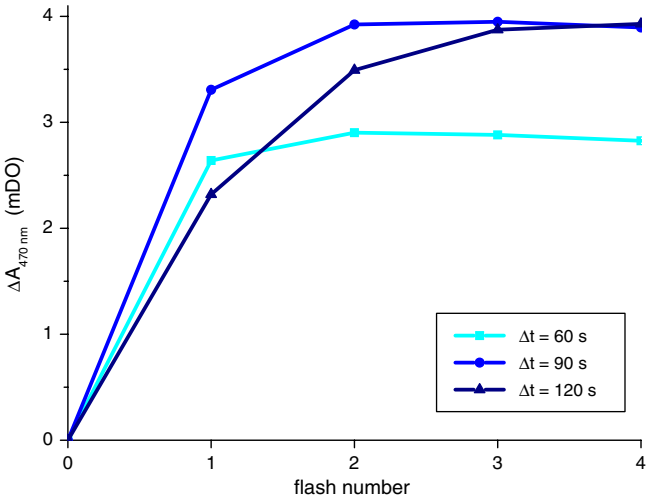

Fig. S3 Progressive oxidation of cytochrome *c* in response to a series of flashes, monitored from the absorption increase at 470 nm. The darker the color the lower the oxygen concentration.

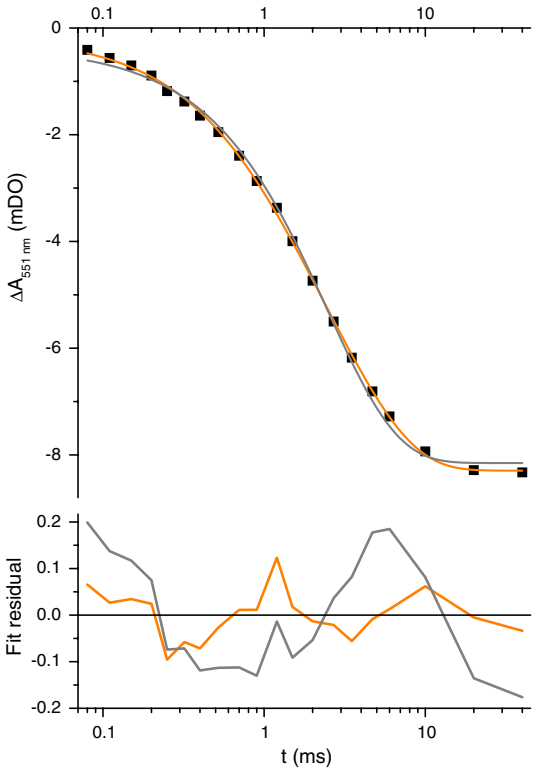

Fig. S4 Kinetics at [O2] = 156 μM of cytochrome *c* oxidation in the W303 Δ*crd1* mutant strain, with monoexponential (gray line) and biexponential fits (orange line) of the data, with the corresponding residuals shown below.

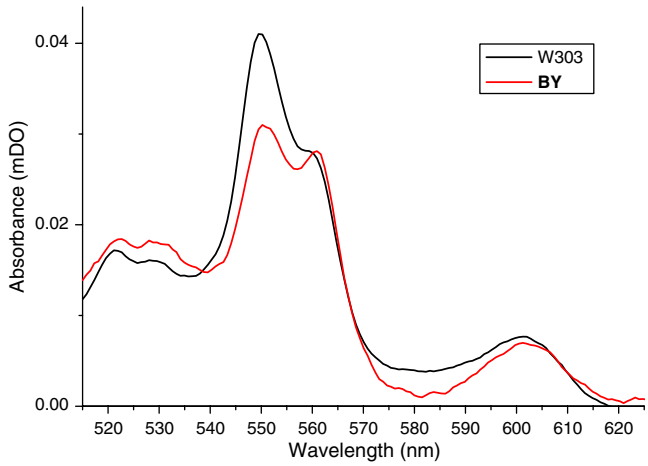

Fig. S5. Absolute spectra of anaerobic suspensions of W303 (black line) and BY (red line) whole cells. Spectra were arbitrarily corrected for scattering and normalized to the amplitude of CcOx.

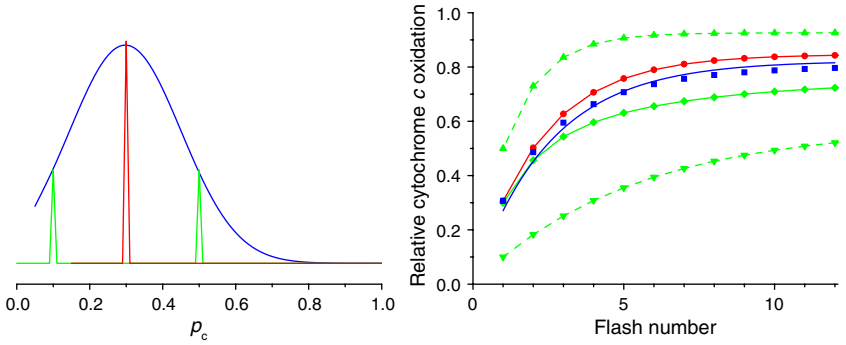

Fig. S6 (Left): Schematic representation of narrow distributions of p_c, at the average value $p_c = 0.3$ (red curve), or at two separate values of $p_c = 0.1$ and $p_c = 0.5$ (down and up triangles respectively), the solid green curve (diamonds) displays the average of these two cases. An intermediate situation, showing a Gaussian distribution of p_c centered at $p_c = 0.3$, is also shown (blue curve). (Right): Simulation of the progressive oxidation of cytochrome *c* upon a series of flashes following a geometric probability law with parameters corresponding to the different cases depicted in (*A*) with the same color codes. The dashed green lines represent the sequential oxidation of cytochrome *c* in the cases $p_c = 0.1$ (down triangles) and $p_c = 0.5$, while the solid green line stands for the average of these two cases. The blue line is a fit of the Gaussian distribution with a single geometric law, including α: $\chi(n) = \sum_{k=0}^{n-1} p_c[(1-\alpha)(1-p_c)]^k$. Notably, the quality of the fit of the simulated data is worse than that of the experimental data (see Fig. 5 or Fig. S7) thus showing that if a Gaussian were to be considered, its width would be narrower than in the case illustrated here. To illustrate the fact that the geometrical profile of sequential oxidation of cytochrome *c* by CcOx demonstrates its ability to freely diffuse, we simulated the consequences of various situations. We suppose that any diffusion-constraining compartment, whether supercomplex or membrane domain, will allow unconstrained diffusion of cytochrome *c* within its own boundaries, and that oxidation of cytochrome *c* will follow a geometrical law in each compartment. The restriction to diffusion is expected to translate into a distribution of p_c values, at a given laser intensity and oxygen concentration. In contrast, free diffusion of cytochrome *c* will result in a single, average value of p_c. We hereby chose to use an average value of p_c of 0.3, meaning that 30% of the cytochrome *c* are oxidized on a single flash, if its diffusion is homogeneous. On the other hand, we compare an extreme case with two compartments being respectively characterized by $p_c = 0.1$ and $p_c = 0.5$ (thus keeping the average p_c equal to 0.3). As a more realistic model, we consider the case of a Gaussian distribution for p_o, again with an average value of $p_c = 0.3$ (left). The consequences of such distributions among compartments on the probability of cytochrome *c* oxidation can be seen in the figure on the right, where the inhomogeneous models always deviate from the plots of the geometrical progressions.

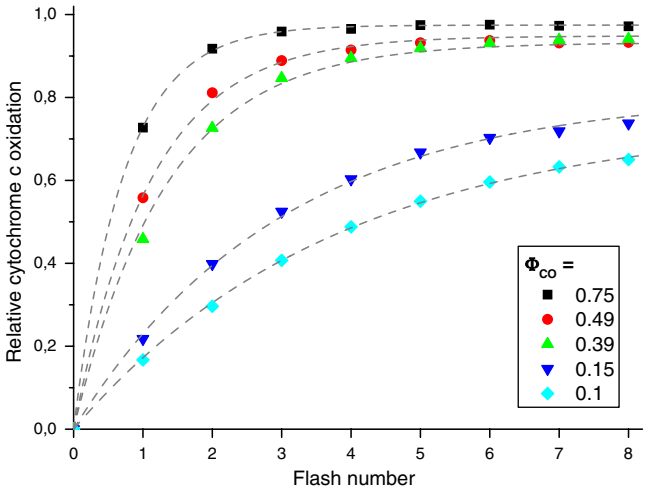

Fig. S7 Relative amount of cytochrome *c* oxidized on a series of flashes at different laser intensities (Φ_{CO}), monitored at 551 nm, in the W303 Δ*atp20* mutant strain. The data processing and legends are the same as for the wild-type strain, displayed in Fig. 5.

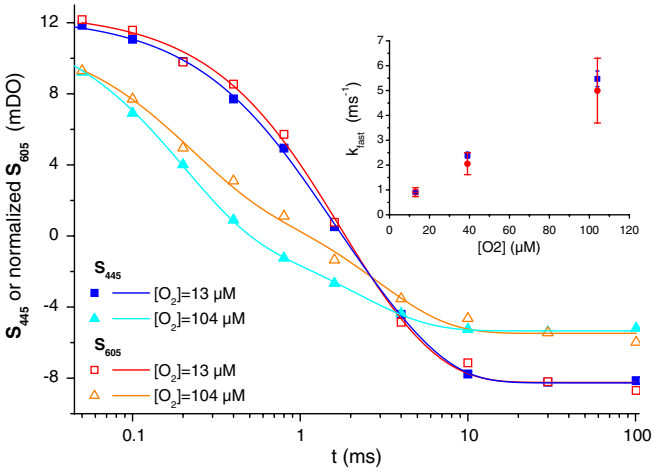

Fig. S8 Kinetics of CcOx oxidation in the W303 strain, monitored at 445 nm and 605 nm, and deconvoluted as described in *Material and Methods* see main text. Data were fitted with biexponential functions (solid lines). The S_{605} curves were arbitrarily normalized by a constant factor in order to match the S_{445} curves. *Inset*: Plot of the rate constant of the fast phase against O_2 concentration, for the S_{445} (blue symbols) and S_{605} traces.